Design of a Portable Fuel Fired Cylindrical TPV Battery Replacement

Lewis Fraas, James Avery, and Leonid Minkin
JX Crystals Inc, Issaquah, WA 98027

A novel portable fuel fired cylindrical thermophotovoltaic battery charger is described. It uses an array of GaSb TPV cells along with a novel Omega recuperator design and a novel IR emitter design. Computational fluid dynamic (CFD) calculations are presented for this TPV cylinder design showing the potential for an overall fuel to electricity conversion efficiency of 10.9%. The estimated weight of the TPV cylinder is 200 gm and its volume is 900 cc. Fuel volume is arbitrary, but a comparable 900 cc of fuel will weigh 540 gm. The specific energy in a hydrocarbon fuel is 12,900 Wh/kg, resulting in 6970 W-hr of energy in the 900 cc tank. The weight of the TPV cylinder and the fuel cylinder combined is thus 740 gm. Given a TPV conversion efficiency of 10%, the converted energy available from the fuel will be 697 W-hr. The specific energy for this TPV system will then be 697 W-hr/0.74 kg = 942 W-hr/kg. A lithium ion rechargeable battery weighing 1.1 kg has a specific energy of 145 W-hr/kg, The TPV power system described here is lighter, has 6.5 times higher specific energy, operates 7 times longer, and is easily refueled.

Nomenclature

PV	=	Photovoltaic
TPV	=	Thermophotovoltaic
η_{TPV}	=	TPV system efficiency
η_{CR}	=	Chemical to radiation conversion efficiency
η_{SP}	=	Spectral efficiency (% radiant energy in cell response band)
η_{PV}	=	PV cell conversion efficiency
VF	=	PV cell view factor (% radiation hitting PV cells)
I_{sc}	=	PV circuit short circuit current
V_{oc}	=	PV circuit open circuit voltage
I_{mp}	=	PV circuit current at maximum power
V_{mp}	=	PV circuit voltage at maximum power
FF	=	PV circuit fill factor = (I_{mp} V_{mp}) / (I_{sc} V_{oc})
IR	=	Infrared

I. Introduction

The first high efficiency low bandgap infrared (IR) sensitive photovoltaic cell, the GaSb cell, was invented and demonstrated by Fraas and Avery in 1989 [1, 2, 3]. This cell responds out to wavelengths of 1.8 microns and enables the use of man made hydrocarbon fuel sourced IR radiators operating at temperatures up to 1700 K for the fabrication of thermophotovoltaic (TPV) DC electric generators. The invention of this cell inspired a renewed surge in TPV system development starting in 1990.

The work on TPV at JX Crystals (JXC) from 1990 up to 2007 is summarized in the TPV-7 conference proceedings [4]. The development of a complete TPV system has required more than just the IR cell. An important additional area of development has included spectral control [5]. It is important to tailor the IR spectrum from the radiant heat source such that the photon wavelengths arriving at the cell fall within the convertible wavelength band for the cell. Longer wavelength radiation falling outside the cell conversion band will simply heat the cell. For this purpose, JXC has developed and patented Cobalt and Nickel doped ceramic matched IR emitters [6, 7].

The TPV work at JXC up until recently has focused primarily on hydrocarbon fired combined heat and power systems for the home. Two such examples are the TPV Midnight Sun Stove [8] and the integration of TPV into a

standard heating furnace [9].

This paper describes a more immediate TPV application: a portable fuel fired cylindrical TPV battery charger or battery substitute. It uses an array of GaSb TPV cells along with a spectrally matched IR emitter and a novel Omega recuperator. Currently, the military carries heavy batteries. The portable cylindrical TPV unit described here is potentially lighter, runs longer, and is more easily recharged (refueled) when compared with a battery. This paper describes the overall TPV cylinder design along with the novel recuperator design and modeled thermal performance. A matched emitter design and the spectral control requirement are also described here.

There was an earlier effort to develop a portable fuel fired TPV battery charger that ended in 2001 (10, 11). That effort was instructive and will be reviewed here with the more recent improvements highlighted.

II. Portable TPV Battery Concept

A. Background

A lithium ion rechargeable battery weighing 1.1 kg has a specific energy of 145 Wh/kg. Meanwhile a hydrocarbon fuel such as Butane or Propane has a specific energy of 12,900 Wh/kg. Therefore, given a small, efficient and lightweight chemical to electrical converter, a much higher specific energy of approximately 1000 Wh/kg should be achievable.

More generally, there is a need for a lightweight compact electric generator that can replace the use of batteries in several potential applications. For example, refueling can be much faster than battery recharging.

B. Overall TPV Battery Design (2010)

Figure 1 shows a perspective view of a portable cylindrical TPV battery charger. It is a cylinder 8 cm in diameter and 15 cm long. There is a cooling air fan on one end and a combustion air fan on the other end. The length from end to end including the two fans is 18 cm. Fuel enters this TPV cylinder and DC electricity is generated. In figure 1, a fuel cylinder is shown adjacent to this TPV cylindrical battery.

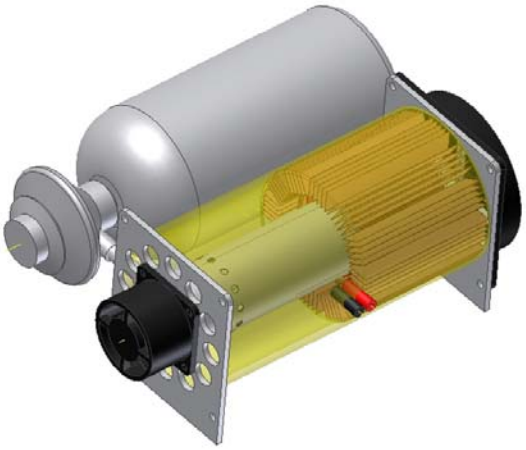

Figure 1: Small portable TPV battery with adjacent fuel cylinder.

C. Concepts

TPV generators are intrinsically lightweight. In a TPV generator, any fuel such as Butane or Propane can be used to heat a small solid element until it glows in the infrared (IR) and photovoltaic cells surrounding the IR emitter simply convert the IR radiation to DC electricity.

Figure 2 shows a cross section drawing of the TPV cylinder shown in Figure 1. The key components and subassemblies are labeled. Referring to Figure 2, one can see the IR emitter subassembly in the middle on the right hand side. It is surrounded by the GaSb TPV cells on a cylindrical circuit with fins for cooling. The power converter array subassembly is cooled via air flow around it from the cooling fan on the cylinder end at the right.

The IR emitter is heated by combustion gases from its inside. Fuel and combustion air are provided through the recuperator as seen on the left hand side.

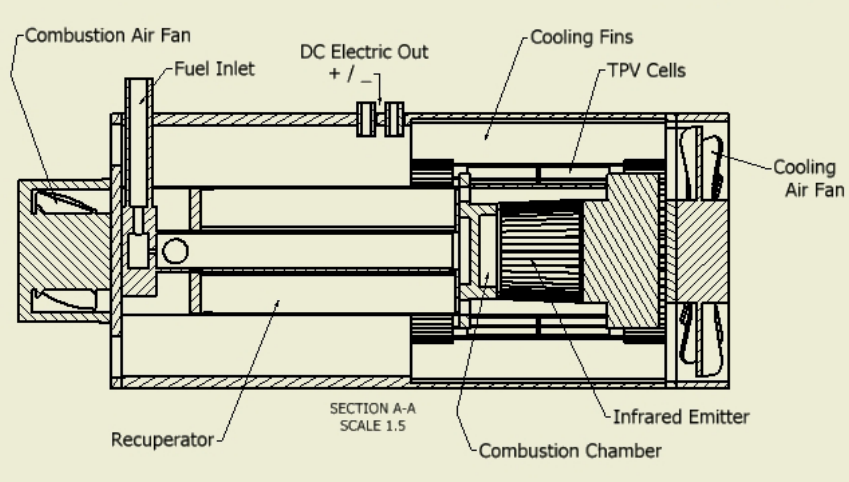

Figure 2: Portable TPV Generator cross section.

A more detailed description is provided in Section III on TPV Subassemblies. The basic principles of operation are described next. Fuel is injected through a metering valve orifice into a Bunsen burner like center coaxial tube. Combustion air is fed into a coaxial space around the fuel tube through a finned recuperator stage and into a fuel and air mixing chamber. A fuel/air swirling mixture is then injected into a combustion chamber and ignited. An IR emitter is located around the combustion chamber. The flame heats the IR emitter to the target temperature of 1200 C (1473 K). The combustion byproduct gases flowing initially in one direction are then turned around and then flow back. These hot exhaust gases are confined by an outer window tube. The exhaust gases now enter the recuperator flowing counter to the combustion air heating the combustion air. The cooled exhaust gases exit the recuperator at the left hand side and mix with the cooling air. TPV cells in circuits surround this combustion / emitter chamber forming the TPV converter section of this compact DC electric generator.

The challenge for TPV is conversion efficiency. However over the last several years, major improvements have been made in TPV converter components.

To first order, the conversion efficiency of a TPV system is given by the product of four terms: the chemical to radiation conversion efficiency, η_{CR} , the percent of radiation in the cell convertible band known as spectral efficiency, η_{SP} , the cell conversion efficiency, η_{PV} , and the cell to emitter view factor efficiency, VF. In recent years, JX Crystals Inc has been making major improvements in all four of these subsystem efficiency areas.

The chemical to radiation conversion efficiency is based on the adiabatic flame temperature of approximately 2000C (2273K) and our IR emitter target temperature of approximately 1200C (1473K). Without provisions to manage the waste exhaust heat, the exhaust temperature would be 1200C and the system chemical to radiation conversion efficiency would only be (2273-1473)/2273 or 35%. This problem is solved by the use of a recuperator where heat from the exhaust gases is extracted and fed back into the combustion air. The recuperator design in this portable cylindrical TPV generator is novel. The goal is to extract 70% of the chemical energy from the fuel and to convert it into radiation.

The goal is to achieve an overall TPV electric conversion efficiency of 10%. TPV cells are now reasonably developed and cell conversion efficiencies for in-band radiation are approximately 30%. In a subsequent section of this paper on the emitter subassembly, spectral efficiency will be discussed with a goal of a spectral efficiency of 60%. Setting a goal for the VF of 80%, then the overall TPV goal efficiency, η_{TPV} , of 10% can be achieved: (The goal of a VF of 80% can be achieved by making the cell area larger than the emitter area in a future TPV circuit design.)

$$\eta_{TPV} = \eta_{CR}\ \eta_{SP}\ \eta_{PV}\ VF = 0.7 \times 0.6 \times 0.3 \times 0.8 = 10\%$$

In the following section, the physical designs of the two primary subassemblies will be described. Then in the section after that, a computational fluid dynamic simulation model will be described. Results from this simulation model are consistent with a 10% overall efficiency prediction.

III. TPV Subassemblies (2010)

The two primary subassemblies are the TPV Power Converter Array and the Burner / Emitter / Recuperator.

A. TPV Power Converter Array

The TPV Power Converter Array subassembly consists of a TPV circuit, cooling fins, and a cooling fan. The GaSb TPV cells and circuits are fabricated at JX Crystals Inc. GaSb cells [1, 12] respond to IR radiation out to 1.8 microns. GaSb TPV cells are mounted on a circuit as shown in Figure 3. The circuit substrate base can be copper or aluminum. This metal circuit base has an insulating layer on its front side coated with a metal layer with a gold reflecting top surface. The top metal layer is etched to create cell pads, circuit traces, and reflective regions as shown.

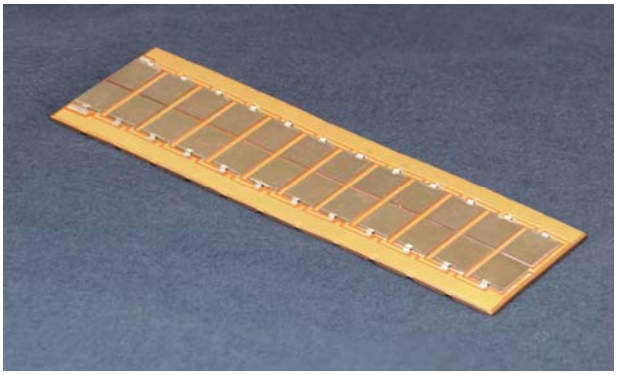

Figure 3: TPV circuit in flat form.

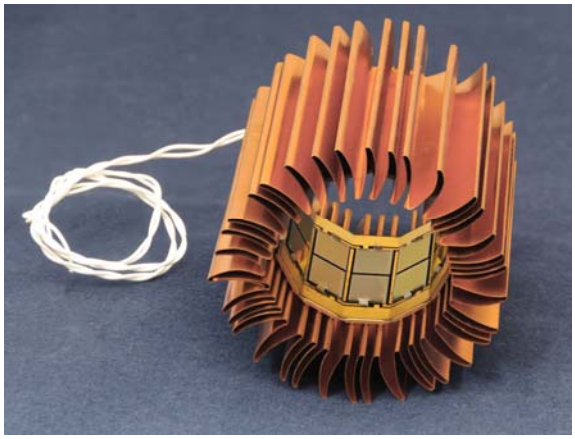

Figure 4: Cylindrical TPV power converter array.

After circuit assembly, this circuit can be flash tested to verify its power conversion performance. After circuit test, convoluted fin stock is then attached to the back side of the TPV circuit. There are machined grooves on the back side of this circuit allowing the circuit to be folded into a polygonal cylinder as shown in Figure 4.

A circuit performance measurement is shown in figure 5.

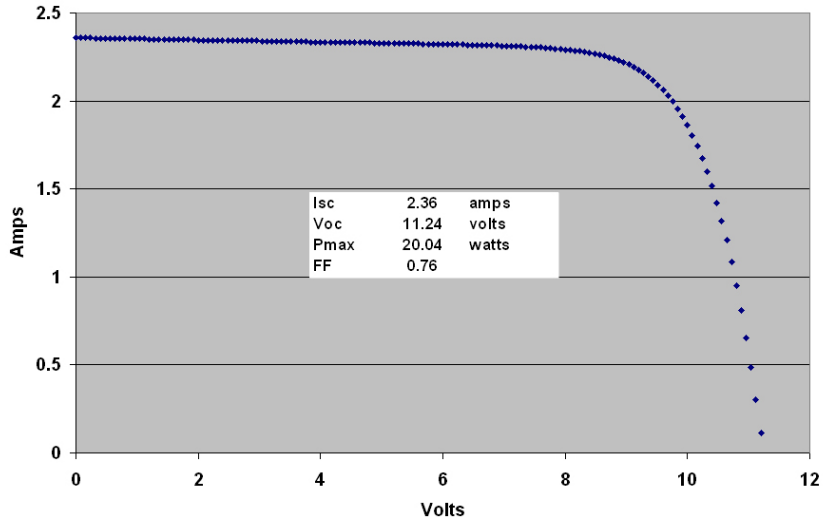

Figure 4: Sample GaSb TPV circuit power curve.

B. Burner / Emitter / Recuperator

A perspective view of the burner / emitter /recuperator subassembly is shown in Figure 6. The IR emitter is shown at the top and the recuperator is shown at the bottom. It divides into a burner / emitter subassembly and a recuperator subassembly. The recuperator and the burner / emitter subassembly are described in more detail in the next sections. The recuperator design and the IR emitter designs are novel and critical to the operation of this TPV generator.

C. Recuperator

The purpose of the recuperator is to extract energy from the exhaust and to transfer that energy into the combustion air stream. Specifically, the goal is to reduce the exhaust temperature from 800 C to 300 C while increasing the combustion air temperature from 20 C to 600 C. The goal is to increase the chemical to radiation efficiency to 70%.through exhaust heat recuperation.

Figure 7 shows front, top, bottom, and cross section drawings of the novel Omega recuperator, and Figure 8 shows a perspective view of the recuperator partially assembled.

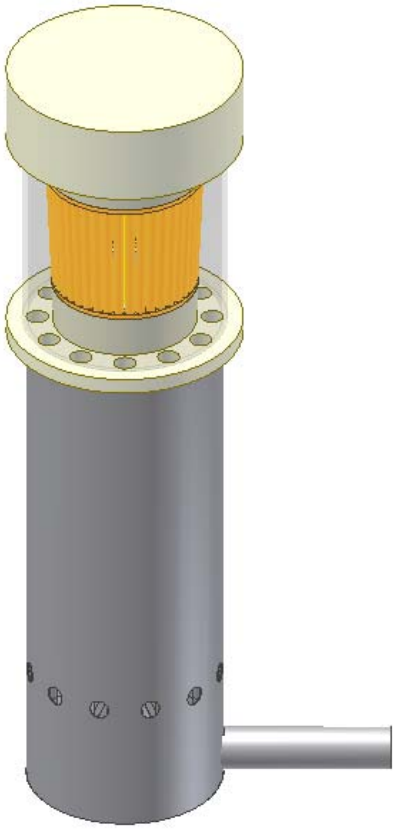

Figure 6: Perspective view of the burner / emitter / recuperator subassembly.

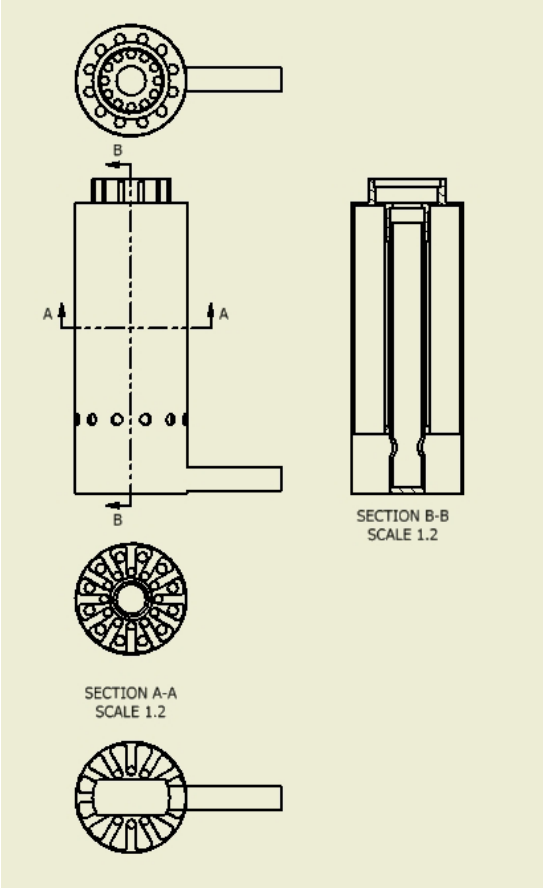

Figure 7: Front, top, and bottom drawings of the Omega recuperator along with horizontal (A-A) and vertical (B-B) cross sections.

The recuperator section is novel in that it uses Omega (Ω) shaped sheet metal heat transfer membranes as shown in Figure 8. A horizontal cross section through this recuperator is shown in section A-A in Figure 7. As shown in this cross section, twelve Omega shaped sheet metal heat transfer elements create alternating flow cavities for the supply combustion air and for the exhaust. Heat transfers through the walls of the Omega shaped elements as air flows in one direction and the exhaust flows in the opposite direction.

Referring to Figure 8, there is a flower shaped disc shown in the upper right. This disc fits over the fuel supply tube and the base of the burner fits over the open end of the fuel supply tube. Figure 8 shows the recuperator

partially assembled. As shown, the Omega shaped sheet metal heat transfer membranes slip into the openings between the petals in the flower shaped disc. One can now see the alternating air supply and exhaust channels. Referring to the top view drawing of the recuperator in Figure 7, one can see two circular hole-patterns. The inner hole-pattern mates with the air channels and allows for the combustion air to enter the combustion chamber. The outer hole-pattern allows for the exhaust to enter the recuperator exhaust channels. Recuperator assembly is completed by placing a cylindrical sleeve around the Omega elements. This sleeve extends down and mates to the combustion air fan. There is a radial hole-pattern in this sleeve shown in Figures 7 that allows the exhaust to exit and mix with the cooling air stream.

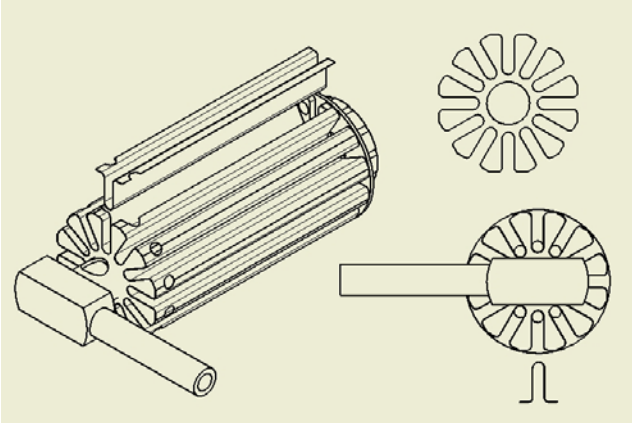

Figure 8: Omega recuperator partially assembled (left); separate drawing of flower disc (top right); bottom view of recuperator (middle right); Cross section through Omega heat transfer membrane (bottom right).

D. IR Emitter

There are three requirements for a good IR emitter design in the context of a fuel fired TPV generator. These requirements are as follows:

1.) It needs to have the appropriate chemical composition such that it emits infrared radiation with wavelengths matched to the response band of the TPV cells.
2.) Its geometry must be such that it efficiently extracts energy from the combustion gases passing through and around it.
3.) It needs to be easily fabricated.

Physical Geometry

Figure 9 shows the side view of the infrared emitter design specifically for the cylindrical TPV generator shown in figures 1 and 2. Figures 10 and 11 show horizontal and vertical cross sections through this burner and IR emitter subassembly.

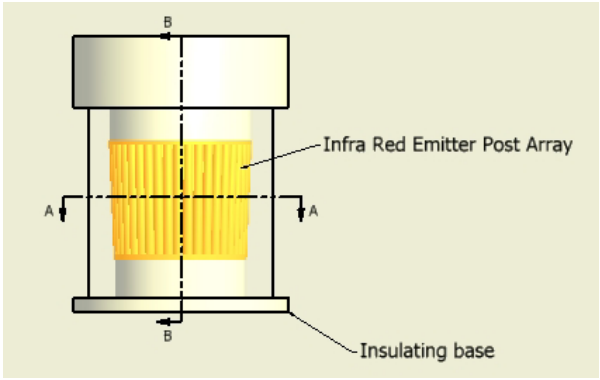

Figure 9: Side view of the Infrared emitter assembly showing the cylindrical array of tilted IR emitter posts and locations of section cuts for figures 10 and 11. The IR emitter rods are shown here as yellow hot.

As shown in figures 10 and 11, the burner and IR emitter subassembly consists of a lower insulating plate with fuel and air injection holes and exhaust gas exit holes. There is a picket fence array of emitter posts on top of this insulating plate with a combustion chamber inside this array. These emitter posts are cylindrical with a diameter of approximately 1 to 2 mm. The hot exhaust gases exit through small slits between these IR emitter posts. The slit widths are approximately 0.1 to 0.2 mm. There is an insulating lid on top of this post array. A sapphire transparent window also surrounds this IR emitter post array. Alternately, a low-OH fused silica window can surround the IR emitter. Because entry and exit holes for both the fuel and air and the exhaust are in the bottom plate, there is a tendency for the lower end of the emitter array to run hotter than the upper end of the emitter array unless the post array is tilted as shown. This tilt increases the slit widths between the emitter posts toward the top end enhancing the heat transfer rate at the top to promote more emitter temperature uniformity from top to bottom.

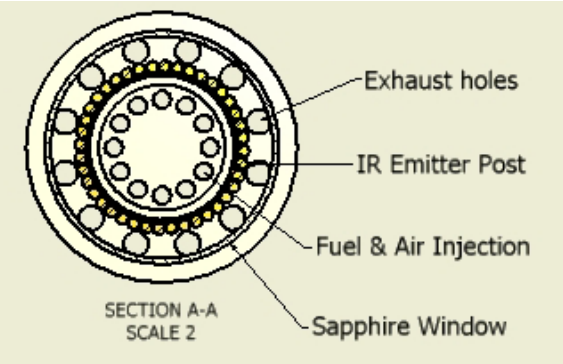

Figure 10: Section A-A through emitter assembly.

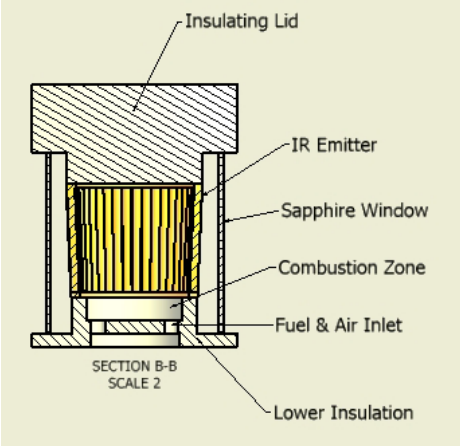

Figure 11: Section B-B through emitter assembly

Chemical Composition

The chemical composition of the IR emitter rods is important for spectral control. The emitter rods needs to have the appropriate chemical composition such that they emit infrared radiation with wavelengths matched to the response band of the TPV cells.

The appropriate TPV cells are either GaSb or InGaAs/InP or Ge cells that convert radiation with wavelengths less than approximately 1.8 microns into electricity. The infrared emitter ideally should only emit radiation with wavelengths less than 1.8 microns. If infrared wavelengths longer than this wavelength are emitted, this radiation will only produce unwanted heat in the TPV cells. It has been shown that Ni or Co ions in an oxide matrix emit radiation in the 1 to 1.8 micron wavelength range [6, 7]. Appropriate IR emitter post for this invention consists of these ions incorporated as impurities in oxide ceramics such as alumina (Al_2O_3, including sapphire), magnesia (MgO), or Spinel ($MgAl_2O_4$),

E. Spectral Control

In section IIC, it was noted that a target spectral efficiency for the IR emitter of 60% would allow a overall TPV efficiency of 10% to be achieved.

It has been shown that Ni or Co ions in an oxide matrix emit radiation in the 1 to 1.8 micron wavelength range [6, 7]. Appropriate IR emitter post for this invention consists of these ions incorporated as impurities in oxide ceramics such as alumina (Al_2O_3, including sapphire), magnesia (MgO), or Spinel ($MgAl_2O_4$),

Ferguson and Dogan [13] have fabricated NiO doped magnesia ribbons for use in TPV generators and measured their spectral emissivity as shown in figure 12.

From the emittance data presented in figure 12, the spectral efficiency can be calculated as shown in Table 1. The radiance numbers presented in this table assume an emitter temperature of 1500 K surrounded by a sapphire window shield at 1000 K. These temperatures are consistent with the values assumed in the overall cylindrical TPV generator model presented in IIC. The resultant spectral efficiency is found to be 61% consistent with the target value.

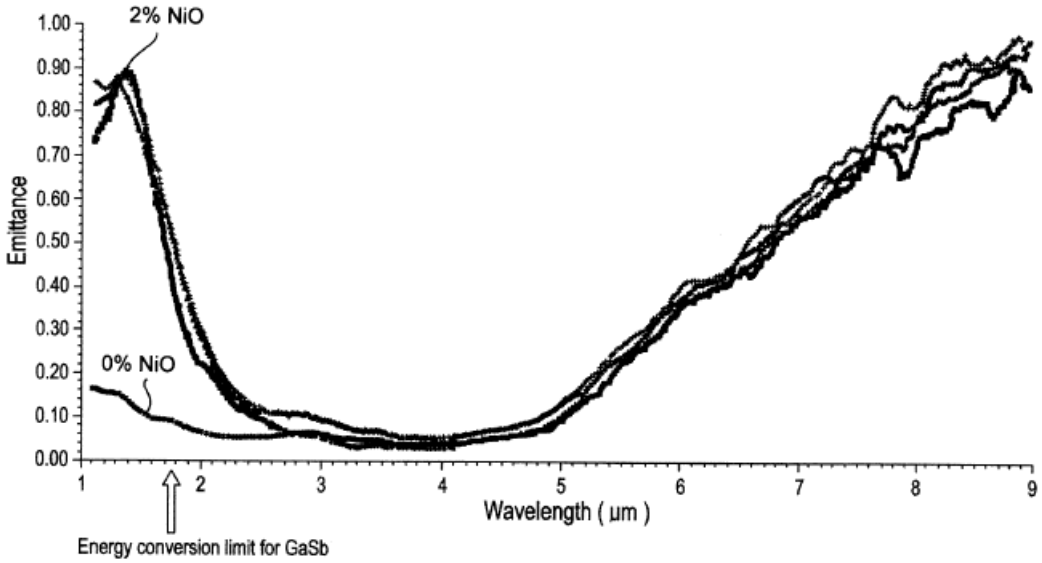

Figure 12: Spectral emittance measurements for a 2 wt.% NiO-doped MgO tape cast ribbon at 1268, 1341, and 1404°C. The emissivity of the 2 wt.% NiO-doped MgO emitter appears nearly constant within this temperature range. The emittance of an 'undoped' MgO ribbon is also included for comparison. The emissivity of the NiO-doped MgO is much greater than it is for the 'undoped' MgO at wavelengths less than about 1.9 µm where radiant energy is efficiently converted by photovoltaic cells, however, NiO doping has little or no effect on the emittance at longer wavelengths.This spectral selectivity' is explained in terms of ligand field theory and interactions between dopant ions and coordinating host atoms [13].

Table 1: NiO doped ceramic emitter Spectral Efficiency

Wavelength	Emissivity	Radiance W/cm2	Comment
0.5 to 1.8 µ	0.9	5.3	1500 K
1.8 to 6 µ	0.1	2	1500 K
6 to 20 µ	1	1.4	Shield at 1000 K
Spectral Efficiency = 5.3/8.7 = 61%			

IV. CFD Modeling (2010 Design)

A. Overview

The design of the portable cylindrical TPV generator described in the previous section is the result of an internal research and development activity at JX Crystals Inc. During this internally funded activity, solid models were created for the cylindrical generator and its subassemblies using Solid Works. Given this ground work, JXC then received funding from the US Army Research Lab and from Sandia National Labs to perform computational fluid dynamic CFD) simulations for the model TPV generator using SolidWorks-cfd-flow-analysis-software [14].

B. Model Results (2010)

The CFD software allows one to integrate solid models with sources of air flow and sources of heat to calculate temperature profiles, flow velocities, and heat transfer rates. The calculations include conduction, convection, and radiation effects.

Several CFD simulations have now been run and the most relevant results are presented in Figures 13, 14, and 15 and Tables 2 and 3. All of these runs used the same cooling air fan, combustion air fan, and heat input simulating a fuel burn rate of 225 W. The cooling air fan chosen has dimensions of 80 mm x 80 mm x 15 mm. It consumes 1.2 W and produces an air flow of up to 1 m^3/min and a pressure of up to 22 Pa. The combustion air fan chosen has

dimensions of 40 mm x 40 mm x 20 mm, consumes 0.8 W and produces a pressure of up to 52 Pa. In the simulations, the combustion air flow was set at 0.1 g/s.

TPV Power Converter Array

Figure 13 shows the temperature profile through the Power Converter Array. The color ranges from 38C for sky blue to 68C for orange. Temperatures over 80C are shown as red. Simulation runs were made for 6 and 8 fins per cell with results showing cell temperatures of 65C and 55C respectively.

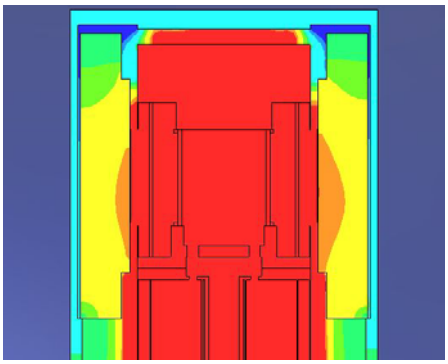

Figure 13: CFD calculation of power converter array temperature profile with 6 fins per cell.

Recuperator

Turning next to the recuperator, figures 14 and 15 show temperature profiles through the recuperator. The colors now range from 20C for blue to red for temperatures above 400C.

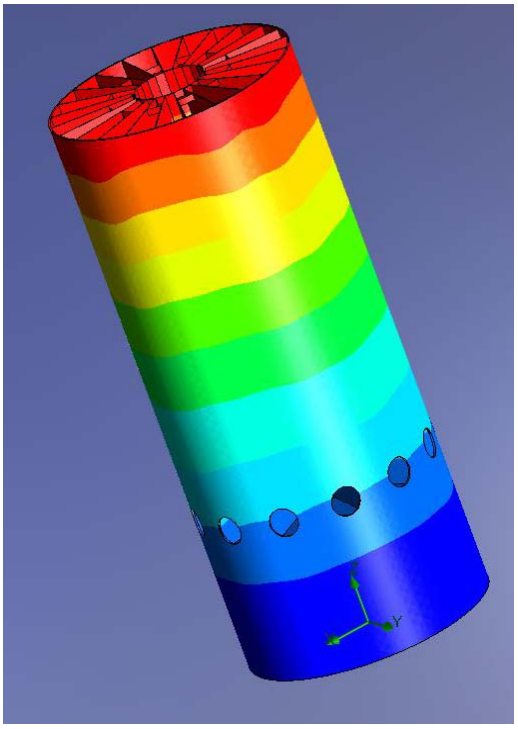

Figure 14: Temperature profile for recuperator.

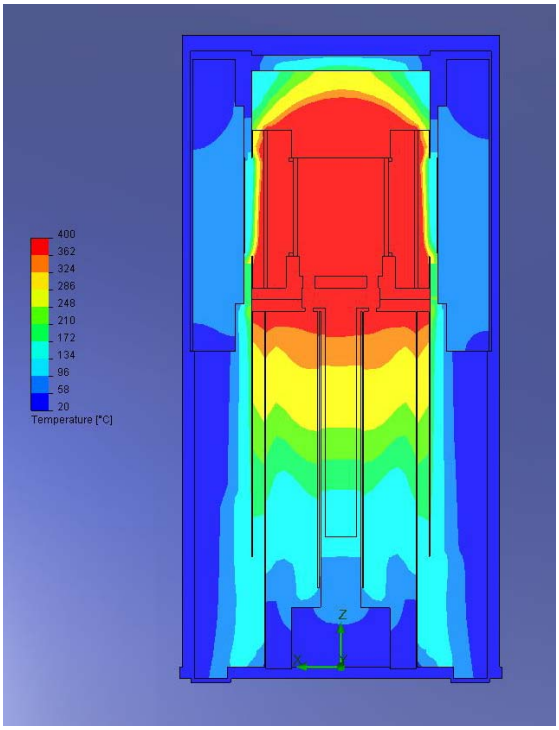

Figure 15: Temperature profile with range from 20 C (blue) to 400 C and above (red).

Referring to Table 3, the solid surface temperature for the recuperator ranged from 120 C to 412 C. The exhaust gas temperature is, of course, somewhat hotter and the inlet air temperature prior to combustion is somewhat cooler.

IR Emitter

Turning next to the IR emitter, Figure 16 shows the temperature cross section profile through the emitter. In the case modeled here, the IR emitter consists of an array of ceramic 2 mm diameter rods with 0.2 mm slits between them. The plan is that these ceramic emitter rods in the TPV generator will be Ni or Co doped matched emitter rods that have wavelength dependent selective emissivity high in the cell converter band and low at wavelengths longer than 1.8 microns.

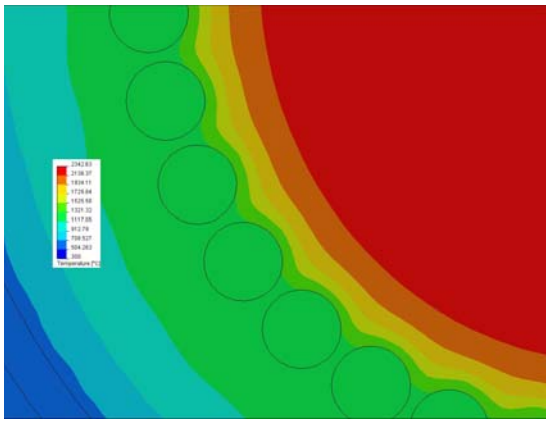

Figure 16: Temperature profile through the 2 mm diameter post array emitter. The color changes occur at 2138, 1934, 1729, 1525, 1321, 1117, 912, and 708 C. Red represents 2138 C temperatures and higher.

However, the CFD software does not allow wavelength dependent emissivity. So, the emitter has been modeled as a gray body with an emissivity of 0.3. This 0.3 value was chosen to match the emitted power over the wavelength range from 0.5 microns to 6 microns for the gray body at 1200C to that projected for a matched emitter over the same wavelength interval at the same temperature. Referring to table 1, the emitted power over this wavelength band at 1200C for the matched emitter should be 7.3 W/cm^2. Since the diameter of the cell array is 48 mm and the diameter of the emitter array is 26 mm, this will correspond to a cell incident power density of 4 W/cm^2. (As noted previously, this reduction in radiant energy flux can be compensated for by increasing the cell receiver area.)

Given the emitter gray body emissivity of 0.3, Figure 16 shows the resultant temperature profile from the CFD simulation. Assuming a combustion gas temperature of 2400C, resulting now from burning preheated air, the IR emitter temperature then reaches 1190C. On the outside of the emitter the gas temperature drops to 800 C.

The result presented in table 1 shows that once the emitter reaches the target temperature, its spectral efficiency will be approximately 60%. However, the emitter geometry must be such that it efficiently extracts energy from the combustion gases passing through and around it so that it reaches the target temperature.

The porosity of the picket fence post array emitter geometry is important. We have now performed computational fluid dynamics (CFD) calculations with the results summarized in table 2 and figure 16. These calculations show that the rod diameter and rod spacing are important for heat transfer. Furthermore, they show that catalytic reactions are not required for efficient heat transfer. This data shows that the gas temperature drops from 2400 C to 1180 C as it passes through the emitter post array leaving the emitter solid temperature at approximately 1190 C suggesting that over 50% of the energy in the gas is extracted as radiation before recuperation.

Table 2: CFD calculation results for emitter post arrays.

	1mm rods	2mm rods	
Temp Solid	1195 avg	1177 avg	°C
Net Radiation	214	219	W
Area	55.76	59.56	cm^2
Pressure	101328-101338	101327-101337	Pa
Radiation Flux	3.95 avg	3.72 avg	W/cm^2
Mass Flow	1.40E-04	1.40E-04	kg/s
Flow Source Temp	2400	2400	°C
Rod spacing	0.1 mm	0.2 mm	
Emitter OD/ID	26/24	28/24	mm
Emitter height	23mm	23mm	

C. Model Projected TPV System Performance (2010)

The results of these portable cylindrical TPV generator CFD simulations are summarized in Table 3. Given a fuel burn rate of 225 W, the model predicts a cell array electrical output of 26.6 W for a gross TPV efficiency of 11.8%. Subtracting the 2 W for the combustion and cooling air fans gives a net TPV system efficiency of 24.6/225 = 10.9%.

Table 3: TPV CFD Simulation Summary

Flow Simulation ID	Jul23-2	Units
Input power	225 W emitter	
emitter temp	1035-1198	°C
combustion air temp	20-2300	°C
combustion air pressure	101325-101378	Pascal
Combustion air mass flow	1.0×10^{-4}	Kg/s
combustion air velocity	0-5.4	m/s
cooling air temp	20-55	°C
cooling air pressure	101325-101350	Pascal
cooling air velocity	0-7.5	m/s
cells net radiant flux	148 W	
Estimated electric with 18% efficiency	26.6 W	
cells net radiant flux density	1.1-5.5, 4.05avg	W/cm^2
cells temperature with 6 fins per cell	65-75, 71avg	°C
cells temperature with 8 fins per cell	55-65, 61avg	°C
recuperator temperature	120-412, 226avg	°C
recuperator sleeve temperature	166-395, 226avg	°C
sapphire temperature	446-581, 527avg	°C
flame temp	501-2339	°C

V. Prior Art Design (2001)

In 1997 through 2001, NASA funded Thermo Power Corporation on a contract entitled "Development and Demonstration of a 25 W TPV Power Source for a Hybrid Power System" [11]. Their TPV concept is shown in figures 17 and 18.

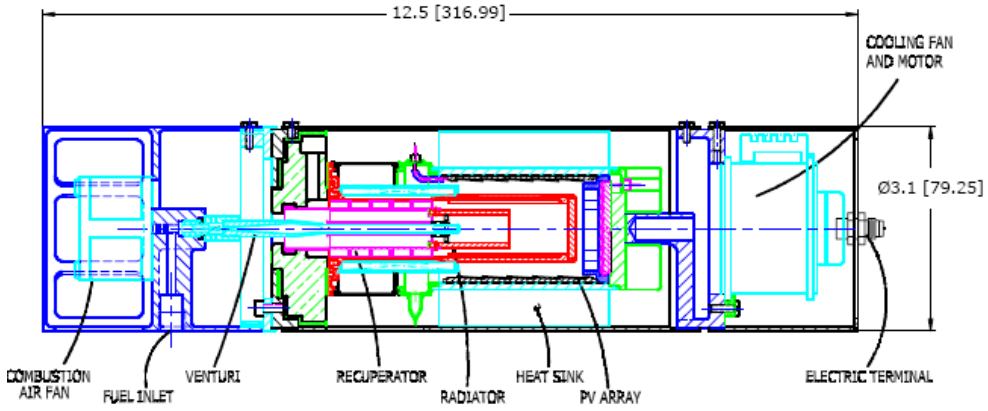

Figure 17: Thermo Power 25 W TPV Design

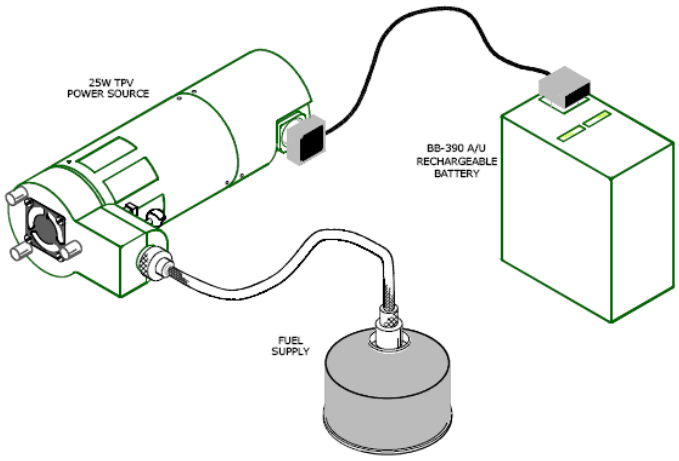

Figure 18: Thermo Power TPV battery charger concept.

This detailed design was a Thermo Power design without input from JX Crystals Inc. Thermo Power then contacted JX Crystals Inc as a component supplier. Working together, a first prototype TPV cylindrical battery charger was built and tested [11]. The 2001 measured results are summarized in Table 4 and contrasted with the 2010 predictions.

Table 4: Performance comparison for 2001 vs 2010.

Subassembly	2001 result	2010 with improved design
Spectral efficiency	31%	60%
Burner, IR Emitter & recuperator efficiency	41%	70%
Power converter array in-band efficiency (In operation)	22.3%	30%
Power converter array in-band efficiency (Uniform illumination)	29.5%	30%
Gross efficiency	3%	11.8%

Today, Thermo Power no longer exists and JX Crystals has revisited this potential application incorporating several improvements. With the benefit of hindsight, several design flaws are evident as reviewed in the following sections.

A. IR Emitter and Spectral Efficiency

Figures 19, 20, and 21 show the details of the Thermo Power burner / emitter (radiator) / recuperator design.

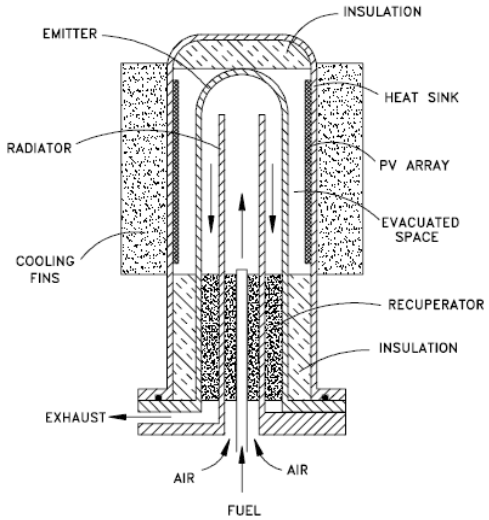

Figure 19: TPV design detail.

Figure 20: AR coated W IR emitter (radiator).

Figure 21: AR coated Pt IR emitter test.

Their initial design utilized an antireflection (AR) coated tungsten (W) emitter along with a multilayer dielectric filter over the TPV cell array for spectral control. However, this design required a vacuum enclosure to avoid oxidation of the tungsten. The initial emitter target temperature was 1700 K. These vacuum and temperature requirements turned out to be too difficult to realize over the course of this contract. So, the actual test runs were done using an AR coated platinum (Pt) emitter without vacuum. However, the peak emissivity of Pt is less than 50%. So the dielectric filter was less effective and the spectral efficiency actually achieved at the test emitter operating temperature of 1460 K was only 31%.

The 2010 design described in sections III D & E above uses a newer NiO doped ceramic oxide emitter design with a higher spectral efficiency of 61%. This design option was developed by an independent group in parallel with the NASA Thermo Power TPV contract but not published until 2001, the year this NASA contract ended. It is simpler and does not require vacuum as required for the AR coated W emitter concept.

B. IR Emitter and Recuperator Design

There are also significant differences in the Thermo Power physical designs for the emitter and recuperator relative to the 2010 picket fence emitter design and the 2010 omega recuperator design. As was noted in section IVB, the porosity of the picket fence post emitter is important for good thermal heat transfer from the combustion gases to the emitter. For example, note in figure 19 for the 2001 design that most of the combustion gases are always several mm away from the emitter rather than passing close to the emitter posts within a distance of 0.1 mm in the picket fence 2010 design. This leads to poor heat transfer efficiency to the emitter for the 2001 design.

The recuperator designs are also significantly different as shown in figure 22.

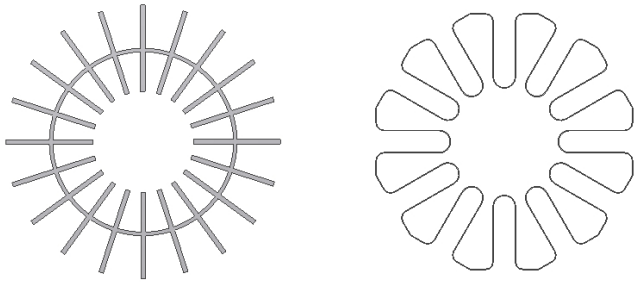

Figure 22: Contrasting recuperator designs.
Left: 2001 design with radial fins. Right: 2010 Omega recuperator design.

Imagine in both recuperator designs that the hot gas is on the outside and the cold gas is on the inside. In the 2001 design, the heat is captured by the outer radial fins and then flows radial along the fins perhaps 5 mm and then the inner radial fins transfer the heat to the colder gas. However in the Omega design, the heat just flows through the 0.1 mm thick membranes. So, the 2010 design is much lighter and more efficient. A problem for the 2001 design is that heat can also flow axially along the fins and cylinder from the hot top end to the cold bottom end of the recuperator and this represent an efficiency loss.

In the 2001 test, the chemical to radiation efficiency was only 41%.

C. Power Converter Array Efficiency

Figure 23 shows the circuits and power converter arrays used in the 2001 NASA TPV activity.

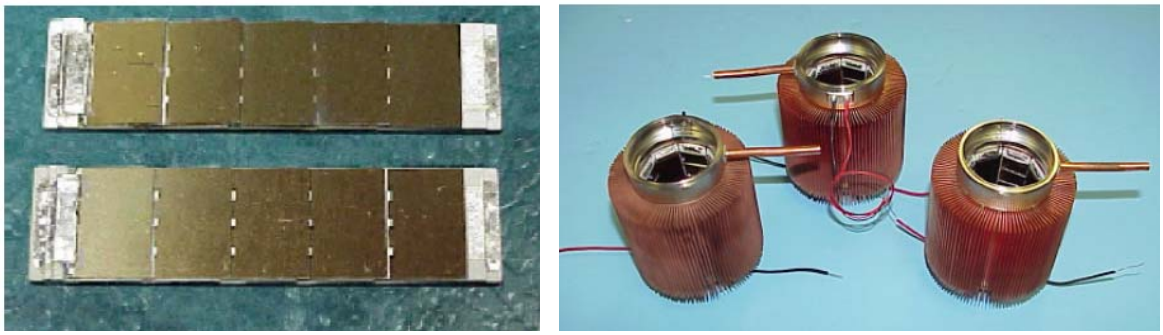

Figure 23: GaSb circuits (left) and TPV power converter arrays (right).

There is an important difference between the 2010 circuit and array design shown in figures 3 and 4 and the 2001 circuit and array design shown in figure 23. The cells in the 2010 circuit are wired in series around the emitter azimuth whereas the cells in the circuits in figure 23 are wired in series parallel to the emitter cylindrical axis. Since the emitter temperature varied along its axis as shown in figure 21 and since the lowest illuminated cell in a series string limits the circuit performance, the temperature non-uniformity in the 2001 design limited the circuit efficiency to 22.3% as shown in table 4. However, as shown in table 4, independent circuit efficiency measurement with uniform illumination showed a circuit efficiency increase to 29.5% close to our design target for 2010. Finally, note that when the cells are wired in series in the azimuth dimension around the emitter as in the 2010 figure 4 design, then the circuit will be tolerant of axial non-uniformity since the circuit can be positioned to balance the currents in the top and bottom strings.

D. Improvements Summary

As noted in sections V A, B, and C above, there are several distinct improvements incorporated into the 2010 design. As noted in table 4, these improvements translate to a predicted TPV gross efficiency improvement to (60/31) x (70/41) x (29.5/22.3) x 3% = 13.1%. This is in reasonable agreement with our model prediction for the TPV gross efficiency for the 2010 design of 11.8%.

VI. Conclusion

TPV cell device efficiencies of 30% have been demonstrated at JXC with GaSb cells [4]. The argument for 60% spectral control efficiency for a matched IR emitter has been presented. Given a 30% cell efficiency and a 60% spectral control efficiency, then 18% of the radiation arriving at the cell circuit should be converted into DC electricity. The CFD simulation results presented in Table 3 suggest that 148 W of radiant energy will arrive at the cell plane given a 225 W fuel burn rate. This means that 0.18 x 148 W = 26.6 W of DC electric power will be produced. Subtracting the combined electric power consumed by the combustion air and cooling air fans of 1.2+0.8=2 W gives a net produced electric power of 24.6 W for a net energy conversion efficiency of 24.6/225 = 10.9%. This is a very exciting result but at present, it is a model prediction. The next step is a funded effort to produce a physical prototype.

The estimated weight of the TPV cylinder described here is about 200 g. The size of the cylinder is 8 cm in diameter x 18 cm long. Its volume then is 900 cc or 900 ml. If a parallel fuel cylinder of equal size and volume is used, the fuel cylinder will contain about 900 ml of fuel and weigh about 540 g. The specific energy in a hydrocarbon fuel is 12,900 Wh/kg. So the energy in the 900 ml fuel cylinder above will be 6970 Wh. The weight of the TPV cylinder and the fuel cylinder combined will be 740 g. Given a TPV conversion efficiency of 10%, the converted energy available from the fuel will be 697 Wh. The specific energy for this TPV system will then be 697 Wh/0.74 kg = 942 Wh/kg. The TPV system described here is lighter than a Li-ion battery, has 6.5 times higher specific energy, operates 7 times longer, and is much more rapidly refueled.

Acknowledgments

This work was partially funded by a contract from the Army Research Lab and parallel funding from Sandia National Labs. Most of the funding was internal IR&D from JX Crystals Inc.

References

[1] L M **Fraas**, JE Avery, PE Gruenbaum, et al, "Fundamental characterization studies of GaSb solar cells", 22nd IEEE PVSC, Las Vegas (1991) 80.

[2] L M **Fraas**, HX Huang, SZ Ye, S Hui, J Avery, "Low cost high power GaSb photovoltaic cells", AIP 401, 3rd TPV Conference (1997), 33.

[3] L M **Fraas**, VS Sundaram, JE Avery, "III-V solar cells and doping processes", US Patent 5,217,539, (1993).

[4] L.Fraas and L. Minkin, "TPV History from 1990 Until Present and Future Trends", AIP 890, 7th TPV Conference (2007), 17.

[5] L.M. Fraas et al, "Thermophotovoltaic System Configurations and Spectral Control", Semiconductor Sci. Technol. **18**, p. S165 (2003).

[6] **L** Ferguson, **L Fraas,** "Matched infrared emitters for use with GaSb TPV cells", AIP 401, 3rd TPV Conference (1997), 169.

[7] LG Ferguson, LM Fraas**,** "Energy-band-matched infrared emitter for use with low bandgap TPV cells"…US Patent 5,865,906, (1999).

[8] L. M. Fraas et al, "Thermophotovoltaic Furnace-Generator for the Home Using Low Bandgap GaSb Cells", Semiconductor Science & Technology **18**, S247 (2003).

[9] R. Carlson and L. Fraas, "Adapting TPV for use in a standard home heating furnace", AIP 890, 7th TPV Conference (2007), 273.

[10] E. Doyle, F. Becker, K. Shukla, and L. Fraas, "Design of a TPV Battery Substitute", AIP 460, 4th TPV Conference (1999).

[11] E. Doyle, K. Shukla, and C. Metcalfe, "Development and Demonstration of a 25 W TPV Power Source for a Hybrid Power System", NASA/CR-2001-211071, August 2001.

[12] http://www.jxcrystals.com/4sale3.pdf

[13] L. Ferguson, F. Dogan, "A highly efficient NiO-Doped MgO matched emitter for thermophotovoltaic energy conversion", Materials Science and Engineering B83 (2001) 35–41.

[14] http://www.solidworks.com/sw/products/cfd-flow-analysis-software.htm